https://doi.org/10.5194/wes-2024-186
Preprint. Discussion started: 23 January 2025

eawe european academy of wind energy
Open Access WIND ENERGY SCIENCE DISCUSSIONS

On reliability design and code calibration of wind turbine blade bearings under extreme wind conditions

Ashkan Rezaei[1] and Amir Rasekhi Nejad[1]

[1]Department of Marine Technology, Norwegian University of Science and Technology (NTNU), NO-7491, Trondheim, Norway

Correspondence: ashkan rezaei (ashkan.rezaei@ntnu.no)

Abstract. This study presents the reliability analysis of the blade bearing in the ultimate limit state. The National Renewable Energy Laboratory 5 MW reference wind turbine is selected for the study, and the Monte Carlo simulation is used for the reliability analysis and estimation of the probability of failure. The uncertainty in turbulence intensity as well as materials are considered in the reliability analysis. A sensitivity analysis is carried out to evaluate the effect of bearing dimension variation. It is observed that conformity and ball diameter have the most sensitivity in the dimension aspect of reliability. IEC standards, as well as wind conditions in different wind sites around the world, are studied, and it is shown that the probability of failure in blade bearing is higher in most of the wind sites than in sites with IEC standard wind.

1 Introduction

Demand for wind turbines will grow drastically over the next decade, and wind turbines are one of the main keys to meeting the IEA Net Zero Emissions by 2050, as stated in IEA (2023). The efficient operation of these turbines depends on various components, with blade bearings being a critical element. Blade bearings facilitate the smooth rotation of the turbine blades, allowing them to capture the kinetic energy of the wind at different wind speeds while the loads in the turbine don't increase. Blade bearings serve as the connection point between the rotor and the hub, allowing the blades to rotate around the hub. Pitch bearing assembly costs around one percent of the wind turbine Stehly et al. (2023); however, changing the broken blade bearing is costly.

Blade bearing failure consists of different failure modes, including rolling contact fatigue, core crushing, edge loading, ring fracture, rotational wear, fretting, and false brinelling (Andreasen et al., 2022). According to standards and guidelines, it is necessary to perform the calculation of the ultimate limit state (ULS) of bearings employing the static safety factor mentioned in IEC 61400-1 (2019); DNV-ST-0437 (2016); Harris et al. (2009); Germanischer Lloyd (2010); Stammler et al. (2024).

There are numerous studies on the fatigue of the bearings; however, the studies about the blade bearing are not many. Among them, Menck et al. (2020) studied different lifetime calculation methods from the standards and guidelines and compared them to each other, highlighting differences in the methods and their results. There are not many studies analyzing the static safety factor in blade bearings. Keller and Guo (2022) studied the static load rating and safety factor of the blade bearing of a 1.5 MW wind turbine. They compared the ISO 76 (2006) methodology with the National Renewable Energy Laboratory's (NREL's)

https://doi.org/10.5194/wes-2024-186
Preprint. Discussion started: 23 January 2025

eawe european academy of wind energy
Open Access WIND ENERGY SCIENCE DISCUSSIONS

pitch and yaw bearing design guideline (DG03) Harris et al. (2009) and concluded that the DG03 methodology is the same as the ISO 76 (2006) recommendation for applications subjected to shock loads. Rezaei et al. (2023) studied the blade bearing of the 5 MW NREL reference wind turbine and shows the importance of seed number in the turbulence wind model at bearing's life. In another work Rezaei and Nejad (2023), the life of the blade bearing is compared in different wind sites and compared with IEC-designed blade bearings. It is shown that the life at some wind sites would be lower; however, the average wind speed is far below the IEC 61400-1 (2019) categories.

Even though it was shown that the results of wind sites are not the same as those of IECs, it is not clear how reliable the results are as the wind is a stochastic phenomenon. Furthermore, blade bearing reliability is not studied thoroughly, and it is not clear what level of reliability one can obtain with the current design process. It is necessary to understand the level of reliability of any components, as it is standardized in ISO 2394 (2015), ISO 19902 (2020), and ISO 19904-1 (2019) in the offshore industry.

The current paper studies the reliability of the blade bearing at ULS, with a deeper focus on the effect of the wind. Bearing static failure is considered a criterion for the ultimate limit state. ISO 76 (2006) stated that experience shows that a total permanent deformation of 0,0001 of the rolling element diameter at the center of the most heavily loaded rolling element/raceway contact can be tolerated in most bearing applications without the subsequent bearing operation being impaired. The bearing static failure corresponds to such a permanent deformation. This permanent deformation can cause possibly stress concentrations of considerable magnitude and the formation of cavities in the raceways. These indentations, together with conditions of marginal lubrication, can lead to surface-initiated fatigue failure [Harris and Kotzalas (2006)].

Moreover, a sensitivity analysis on the effect of the bearing's main parameter on the probability of static failure of the blade bearing was performed.

2 Case study: wind turbine and wind sites

2.1 Reference wind turbine

Load calculations were carried out using the NREL 5MW reference wind turbine by Jonkman et al. (2009). It is an offshore wind turbine, designed for wind class IEC IB. The turbine properties are displayed in Table 1.

https://doi.org/10.5194/wes-2024-186
Preprint. Discussion started: 23 January 2025

eawe european academy of wind energy
Open Access WIND ENERGY SCIENCE DISCUSSIONS

Table 1. 5 MW NREL reference wind turbine specification Jonkman et al. (2009)

Wind Turbine	NREL 5 MW Reference Wind Turbine
Rating	5 MW
Rotor Diameter	126 m
Hub Height	90 m
Drivetrain	High-speed, multiple-stage gearbox
Minimum and Rated Rotor Speed	6.9 rpm, 12.1 rpm
Cut-In, Rated, Cut-Out Wind Speed	3 m/s, 11.4 m/s, 25 m/s
Overhang, Shaft Tilt, Precone	5 m, 5°, 2.5°
Rotor Mass	110,000 kg
Nacelle Mass	240,000 kg
Tower Mass	347,460 kg

2.2 Blade bearing

The blade bearing model is considered from work by Rezaei et al. (2023). The bearing is a double-row, four-point contact ball bearing with a total of 250 balls. The general specification of the bearing is presented in Table 2. The details of the bearing specifications and dimensions can be accessed at Rezaei et al. (2023).

Table 2. Blade bearing main dimensions

Parameter	Value	Description
D_{pw}	3558	Bearing pitch diameter (mm)
D	75	Ball diameter (mm)
α	45	Initial contact angle (°)
Z	125	Number of balls per row
i	2	Number of rows
f_i	0.53	Inner raceway groove radius/D
f_o	0.53	Outer raceway groove radius/D

2.3 Wind sites

The wind regimes consist of IEC-category wind fields and wind sites. IEC-category wind fields consist of three wind speed classes: I, II, and III. Each wind speed class has four subclasses of A+, A, B, and C based on turbulence intensity. The basic parameters of the wind turbine classes are presented in Table 3 (IEC 61400-1, 2019). In the table V_{ave} is the annual wind speed, V_{ref} is the reference wind speed average over 10 minutes, and I_{ref} is the reference value of the turbulence intensity.

https://doi.org/10.5194/wes-2024-186
Preprint. Discussion started: 23 January 2025

eawe european academy of wind energy
Open Access WIND ENERGY SCIENCE DISCUSSIONS

Table 3. Basic parameters for IEC-category wind turbine IEC 61400-1 (2019)

Wind turbine class	I	II	III
V_{ave} (m/s)	10	8.5	7.5
V_{ref} (m/s)	50	42.5	37.5
A+, I_{ref}		0.18	
A, I_{ref}		0.16	
B, I_{ref}		0.14	
C, I_{ref}		0.12	

The wind sites include 13 in Iran [SATBA (2022)], Pakistan [World Bank Group (2023b)], Vietnam [GIZ (2023)], Ethiopia [World Bank Group (2023a)], Denmark [Ørsted (2022)], and the United States of America [Jager and Andreas (1996)]. The wind data includes the mean and standard deviation of 10-min wind speed. In order to account for the wind's seasonal effect, data needs to cover an entire year. Nominated wind sites cover a whole year's measurements. More information on the wind sites is presented at work by Rezaei and Nejad (2023).

3 Methodology

3.1 Structural reliability

The study of structural reliability is concerned with calculating and predicting the probability of limit state violation for an engineered system at any stage during its life as defined by Melchers and Beck (2018). Nejad (2018) named the main aim of the structural reliability as an estimation of the failure probability by taking into account explicitly uncertainties of the load, load effect, and resistance.

Ultimate limit state reliability in the current work is based on a static safety factor. The procedure for the ultimate limit state calculated in this paper is illustrated in Fig. 1. In the next section, the procedure for each step is presented.

https://doi.org/10.5194/wes-2024-186
Preprint. Discussion started: 23 January 2025

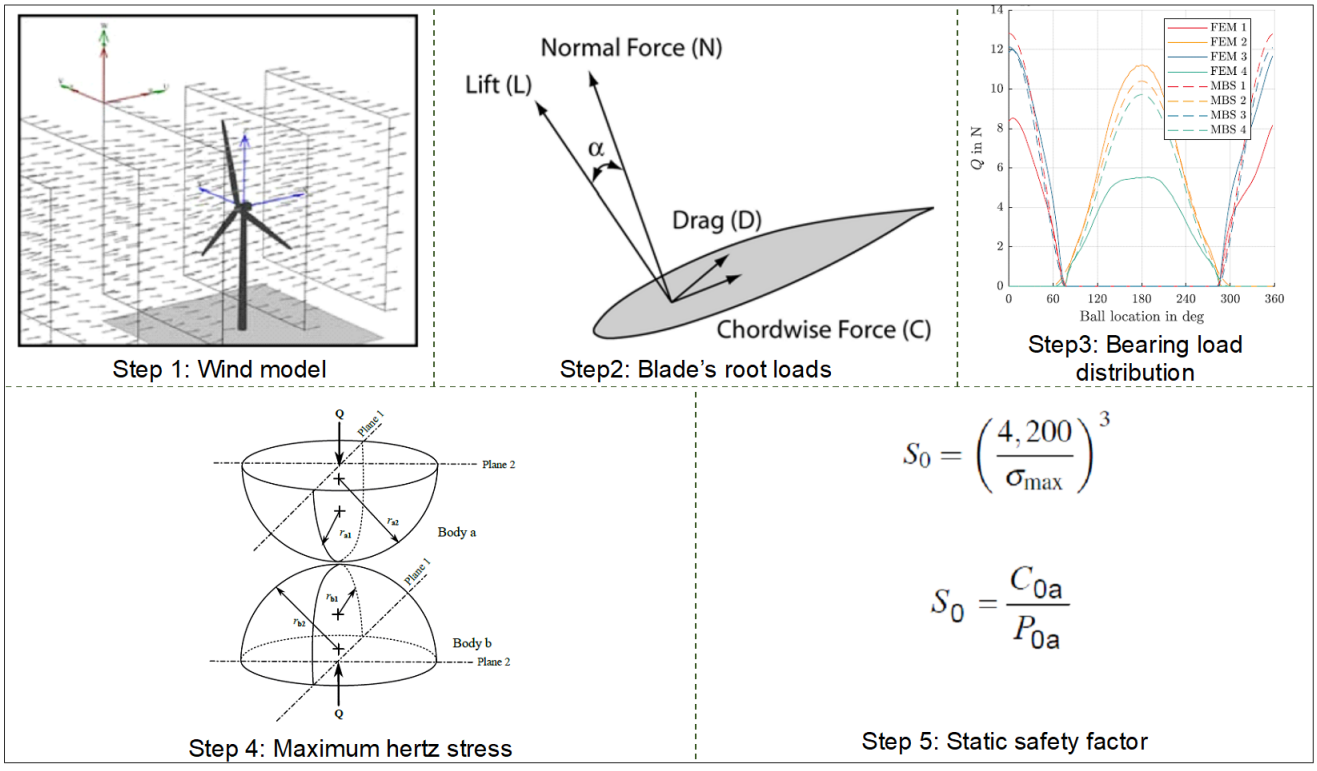

Figure 1. Illustration of the procedure that static safety factor is calculated

https://doi.org/10.5194/wes-2024-186
Preprint. Discussion started: 23 January 2025

eawe european academy of wind energy
Open Access WIND ENERGY SCIENCE DISCUSSIONS

3.2 Safety factor and failure function

A safety factor is a measure used in engineering and design to provide a margin of safety for structures, materials, or systems under expected loads or conditions. It accounts for uncertainties in the design process, such as variations in material properties, manufacturing tolerances, unexpected loads, and potential degradation over time. In this study, the formula that is used for the failure function has the same formation as the static calculation function and static safety factors.

The safety factor, according to ISO 76 (2006), is a ratio between the basic static load rating and the static equivalent load, giving a margin of safety against inadmissible permanent deformation on rolling elements and raceways, and is defined as

$$S_0 = \frac{C_{0a}}{P_{0a}} \tag{1}$$

where C_{0a} is the basic static axial load rating

$$C_{0a} = f_{0a} i Z D^2 sin\alpha \tag{2}$$

and P_{0a} the static equivalent axial load.

$$P_{0a} = 2.3 F_r tan\alpha + F_a \tag{3}$$

f_{0a} is a geometric factor, calculated from Table 1 in ISO 76 (2006). F_a in P_{0a} includes both direct axial force and axial force due to the bending moment on the bearing. Another approach is to consider that bearing static failure occurs when the maximum Hertz contact stress exceeds the allowable Hertz contact stress. In this regard, the static safety factor (SF) is the ratio of the allowable ball load to the actual ball load Harris et al. (2009). The DG03 uses a comparison of the maximum contact stress, σ_{max}, in the limit load condition to the maximum allowable stress of 4,200 MPa to define the static safety factor as Harris et al. (2009) and Stammler et al. (2024)

$$S_0 = (\frac{4200}{\sigma_{max}})^3 \tag{4}$$

where the maximum contact stress, σ_{max}, is also expressed in megapascals calculated as

$$\sigma_{max} = \frac{1.5 Q_{max}}{\pi ab} \tag{5}$$

and the static safety factor can be rewritten as

$$S_0 = \left(\frac{\frac{4200 \pi ab}{1.5}}{Q_{max}} \right)^3 \tag{6}$$

In equation 5, πab is the contact area, which is an ellipse having semi-major axis a and semi-minor axis b, and Q_{max} is the maximum ball force. The maximum ball load is calculated from

$$Q_{max} = 0.55 \left(\frac{2F_r}{Z cos\alpha} + \frac{F_a}{Z sin\alpha} + \frac{4.4M}{D_{pw} Z sin\alpha} \right) \tag{7}$$

https://doi.org/10.5194/wes-2024-186
Preprint. Discussion started: 23 January 2025

eawe european academy of wind energy
Open Access WIND ENERGY SCIENCE DISCUSSIONS

where F_r, F_a, and M denote the applied radial, axial, and moment loads, respectively. D_{pw} denotes the pitch diameter of the bearing. z is the number of balls and α is the contact angle.

In Equation 6, the numerator and denominator are named R and S, respectively. The failure function, g_x, is defined below, where x is random variables and n is the static safety ratio.

$$g_x(R,S) = (\frac{R}{S})^3 \leq n \tag{8}$$

The static safety ratio, n, determines the boundary of the failure. If the failure function value is equal to or greater than the static safety ratio, the bearing is safe; otherwise, the bearing is in a failure state. In a work by Keller and Guo (2022), it is recommended that the static safety ratio be greater than 1.5; however, Stammler et al. (2024) noted that it seems reasonable to refer to the limit of 1 such as IEC 61400-1 (2019). In order to compute the actual reliability and allow for comparisons, the static factor ratio equal to 1 is considered. Consequently, g_x will become

$$g_x(R,S) = (\frac{R}{S})^3 \leq 1 \tag{9}$$

The failure function can be written as

$$g_x(R,S) = R^3 - S^3 \leq 0 \tag{10}$$

and

$$g_x(R,S) = (R-S)(R^2 + RS + S^2) \leq 0 \tag{11}$$

In order to make the failure function negative, one of the two terms in Equation 11 should be negative. The second parenthesis in Equation 11 is always positive, so the first term $(R-S)$ should be negative to make the failure function negative. Therefore, the failure function would be

$$g_x(R,S) = R - S \leq 0 \tag{12}$$

The probability of failure P_f is then obtained from

$$P_f = P(g_x(R,S) \leq 0) = P(R - S \leq 0) \tag{13}$$

To find P_f different methods of the first- and second-order reliability methods (FORM and SORM), and Monte Carlo can be used Ditlevsen and Madsen (2007). Monte Carlo simulation has been used in this paper. By the Monte Carlo simulation method, a suitably large sample of typical load configurations is simulated from the probabilistic action model. This load configuration sample gives a corresponding sample of load effects at different points of the bearing, and from this sample, the probability distributions of the load effects can be estimated. By using these probability distributions, extreme value studies can next be made. In this sense, the probabilistic model uses typical load configurations in its solution procedure and not difficult choices of “extreme" load configurations as they are used in the deterministic model Ditlevsen and Madsen (2007).

https://doi.org/10.5194/wes-2024-186
Preprint. Discussion started: 23 January 2025

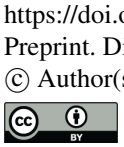

WIND ENERGY SCIENCE DISCUSSIONS

The randomness of the failure function arises from different aspects. Uncertainties in material, forces, and models are some of the main ones. These randomnesses can appear in the R or S or both, which represent the resistance and stress due to external loads in the bearing, respectively. The randomness in resistance and stress in the current work originated from uncertainty in the materials, dimensions, wind turbulence intensity, and simulation model in ball forces. In Fig. 2 a systematic approach for the reliability analysis of a blade bearing is presented.

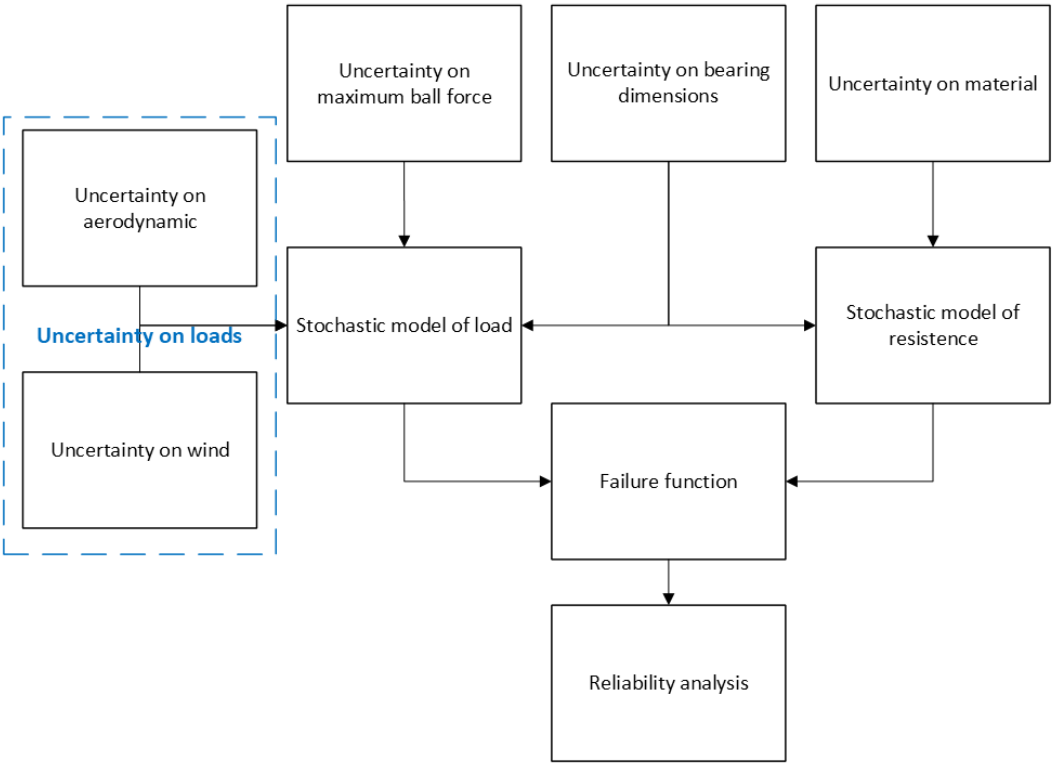

Figure 2. Flowchart of reliability analysis in a blade bearing for ultimate limit state

Uncertainty in material leads to uncertainty in resistance, while uncertainty in dimension leads to both uncertainty in stress and resistance. The formula for resistance extracted from Equation 14 with consideration of uncertainty in material and dimension presented below,

$$R = \left(\frac{4200 \chi_m \pi a(\chi_d) b(\chi_d)}{1.5} \right) \tag{14}$$

where χ_m and χ_d are uncertainty in material and dimension, respectively. Uncertainty in dimension has an effect on the dimension of the contact area, a and b. It should be noted that a and b are, in addition to the uncertainty in dimension, functions of uncertainty in the loads and the maximum ball forces. The formula that represents S, presented below,

$$S = (Q_{max} \chi_f) \tag{15}$$

https://doi.org/10.5194/wes-2024-186
Preprint. Discussion started: 23 January 2025

where χ_f is uncertainty in maximum ball force. Q_{max} contains external loads and bearing dimensions, which in fact are uncertain parameters. Therefore, in its nature, it consists of uncertainty.

The probability of failure including all uncertainties will then be

$$P_f = P\left(\left(\frac{4200\chi_m \pi a(\chi_d) b(\chi_d)}{1.5}\right) - (Q_{max}\chi_f) \leq 0\right) \tag{16}$$

3.2.1 Uncertainty in material

The strength of bearings is not a deterministic value. ISO 76 (2006) recommends a Hertz contact stress of 4200 MPa for ball bearings, which is equivalent to a total permanent deformation of 0.0001 of the rolling element diameter. Assessing the uncertainty of the material's strength requires extensive testing. Shimizu et al. (2010) presented the mechanical properties of the AISI 52100 bearing steel. They showed that tensile strength and Rockwell C hardness have a normal distribution with a standard deviation of 5.7% and 1.1%, respectively. Lewis et al. (2015) assessed 9 different sources, including 7 bearing manufacturers, and allowable peak Hertzian pressures of 4270 MPa and 3962 MPa for SAE 52100 steel and AISI 440C steel, respectively, based on the mean minimum hardness. Wang and Zhang (2022) performed a reliability analysis on an angular contact ball bearing. They considered allowable yield stress as a strength parameter with a 5% standard deviation. In another work, density and module of elasticity in work by Cheng et al. (2020) is considered a normal distribution with a 5% standard deviation. In their sensitivity analysis, they concluded that the material has the highest reliability sensitivity. The current work considered a normal distribution with a standard deviation of 5.7% for uncertainty of material, χ_m.

3.2.2 Uncertainty in dimensions

Blade bearing dimensions affect the loads and resistance in the failure function. Wang and Zhang (2022) performed a sensitivity analysis on four parameters of the bearing, including ball pitch diameter, ball diameter, and inner and outer raceway groove curvature with normal distributions and 0.5% standard deviations. They concluded that, regarding the bearing geometry, the ball diameter has the highest effect on reliability to prevent plastic deformation. Cheng et al. (2020) sensitivity analysis on an angular contact ball bearing, free contact angle, and inner and outer raceways were considered random parameters apart from ball diameter and groove curvatures. All of their random parameters had 0.5% standard deviations. In a reliability and sensitivity analysis of spherical roller bearings, Wang et al. (2020) considered 4%, 2.2%, and 0.5% standard deviation for ball diameter, pitch diameter, and radial clearance, respectively. The effect of dimensions on reliability of the bearing is presented in the sensetivity analysis section.

3.2.3 Uncertainty in loads

Wang and Zhang (2022), in their work, considered normal distributions with a 5% standard deviation for axial and radial forces. The same consideration at work by Cheng et al. (2020) has been seen. In contrast, Wang et al. (2020) considered a standard deviation of 2.5% for the radial load.

https://doi.org/10.5194/wes-2024-186
Preprint. Discussion started: 23 January 2025

eawe european academy of wind energy
Open Access WIND ENERGY SCIENCE DISCUSSIONS

The uncertainty of the load at the blade bearing originates mainly from the turbulence of the wind turbine, and the turbulence has a great contribution to both the safety factor and the life of the blade bearing, as shown in the work by Rezaei et al. (2023). Different realizations of the turbulence intensity were considered with different random seed numbers. Different seed numbers produce a Gaussian distribution of TI in the longitudinal wind component, due to the spatial coherence. In other words, seed numbers are used to create random phases (one per frequency per grid point per wind component) for the velocity time series in the turbulence wind model Jonkman (2009).

Each simulation with a specific seed number leads to a time series of distributions of the loads in the balls, while the extreme ball load can be obtained from these series. Different random seed number simulations result in a series of extreme ball loads in the blade bearing while the turbulence intensity is constant. These extreme loads form a probability distribution function. It is important to assign a proper probability distribution function to these extreme loads.

In this study, probability distribution functions of generalized extreme value, Gamma, inverse Gaussian, Kernel, lognormal, Nakagami, Rician, and Weibull were considered. In Table 4, the probability density function (PDF) of the nominated distribution function is presented, where x is a random variable. More information on the equations and parameter definitions of generalized extreme value, Gamma, Kernel, and Weibull is referred to in Shi et al. (2021). The parameters of inverse Gaussian, lognormal, and Nakagami are referred to in Alavi et al. (2016). Rician parameters are referred to in Yu et al. (2019).

Table 4. PDFs of nominated distribution function Alavi et al. (2016); Shi et al. (2021); Yu et al. (2019)

Distribution function	PDF
Generalized Extreme Value (GEV)	$f(x) = \frac{1}{\alpha}[1 - \frac{k}{\alpha}(x-\mu)]^{\frac{1}{k}-1} - e^{-[1-\frac{k}{\alpha}(x-\mu)]^{\frac{1}{k}}}$
Gamma (Gam)	$f(x) = \frac{\alpha^k}{\Gamma(k)} x^{k-1} e^{-\alpha x}$
Inverse Gaussian (IG)	$f(x) = \sqrt{\frac{\lambda}{2\pi x^3}} e^{-\frac{\lambda}{2\mu^2 x}(x-\mu^2)}$
Kernel (Ker)	$f(\alpha) = \frac{1}{nh}\sum_{i=1}^{n} K(\alpha), \quad \alpha = \frac{x-x_i}{h}$
Lognormal (LN)	$f(x) = \frac{1}{x\sigma\sqrt{2\pi}} e^{-\frac{1}{2}[\frac{ln(x)-\mu}{\sigma}]^2}$
Nakagami (Nak)	$f(x) = \frac{2m^m}{\Gamma(m)\Omega^m} x^{2m-1} e^{-\frac{m}{\Omega}x^2}$
Rician (Ric)	$f(x) = \frac{x}{a^2} e^{-\frac{x^2+b^2}{2a^2}} I_0(\frac{bx}{a^2})$
Weibull (Wbl)	$f(x) = \frac{k}{\alpha}(\frac{x}{\alpha})^{k-1} e^{-(\frac{x}{\alpha})^k}$

In this study, the parameters were calculated by the maximum likelihood estimator Bain and Antle (1967) using MATLAB software, and to assess the performance and goodness-of-fit (GoF) of the distribution functions, the coefficient of efficiency method (CE) has been applied. CE is intended to range from zero to one, but negative scores are also permitted. The maximum positive score of one represents a perfect model; a value of zero indicates that the model is no better than a one-parameter "no knowledge" model in which the forecast is the mean of the observed series at all time steps; negative scores are unbounded; and a negative value indicates that the model is performing worse than a "no knowledge" model according to Dawson et al. (2007). The CE indicator is one minus the ratio of the sum square error to the statistical variance of the observed dataset about

https://doi.org/10.5194/wes-2024-186
Preprint. Discussion started: 23 January 2025

the mean of the observed dataset.

$$CE = 1 - \frac{\sum (Q_i - \hat{Q}_i)^2}{\sum (Q_i - \bar{Q})^2} \tag{17}$$

Q_i is observed data at level i, $\hat{Q}_i$ is estimated data at level i, and $\bar{Q}$ is the mean of observed data.

Different seed numbers were studied to create a distribution function. According to IEC 61400-1 (2019), in ultimate strength analysis, 15 different simulations are necessary for each wind speed from $(V_r - 2m/s)$ to cut-out, and six simulations are necessary for each wind speed below $(V_r - 2m/s)$. However, for generating coherent turbulent structures, using more than 30 different random seeds for a specific set of boundary conditions is recommended by Jonkman (2009). This study covers a wide range of seed numbers. The generalized extreme value is considered for the maximum load distribution function. The reason behind is presented in the results section.

3.2.4 Uncertainty in the maximum ball force

The uncertainty in the maximum ball forces arises from the distribution of the forces inside bearings. The flexibility of the bearings and connecting components, hub and blade, can affect the load distributions inside the bearing, as were shown in works by Menck et al. (2020) and Rezaei et al. (2024). In addition, the results of the maximum ball force equation are not necessarily conservative. It can overestimate or underestimate the actual loads Stammler et al. (2024).

Menck et al. (2020) developed a finite element model (FEM) and calculated the bearing load distributions. Moreover, Graßmann et al. (2023) validated the finite element model with extensive experimental data on the blade bearing. Furthermore, Rezaei et al. (2024) compared the load distribution from the finite element model and multi-body simulations (MBS) for NREL 5MW and IWES 7.5 MW wind turbines. The average of the maximum ball force differences between MBS and FEM was 10.8%. In another work by Leupold et al. (2021), load distributions inside the bearing for two different conditions of finite element and multi-body simulation were studied, and the average error was 6.5%.

The maximum ball forces and load distributions in the work by Rezaei et al. (2024) were recalculated with the maximum ball force equation. The differences between the maximum forces from FEM and the maximum ball equation have a mean and standard deviation of 13% and 6.5%, respectively, which is considered an uncertainty of maximum ball forces, χ_f.

The distributions and the mean and standard deviation of model uncertainties based on the above discussions are summarized in Table 5.

Table 5. Uncertainty distributions

Uncertainty	Distribution	Mean	St. dev.
χ_f	Normal	1.13	0.065
χ_m	Normal	1	0.057
χ_d	Normal	1	0.005
Q_{max}	GEV	Distribution depends on each wind conditions	

https://doi.org/10.5194/wes-2024-186
Preprint. Discussion started: 23 January 2025

3.3 Description of DLC

It is observed that design load case (DLC) 1.3 of IEC 61400 around rated wind speed has the largest effect on the load of the blade bearings Rezaei et al. (2023); therefore, it is considered a nominated load case.

The DLC 1.3 contributes to an extreme turbulence model (ETM). DLC covered the mean wind speed from 10 to 13 m/s with an interval of 0.5 m/s. The simulations last 700 seconds, and the results of the first hundred seconds are not considered. In all DLCs, wind shear is considered according to the sites or related standard conditions.

4 Results and discussion

4.1 Probability distribution function

Seed numbers from 15 to 3000 were studied in onshore wind conditions in IEC category IA. The results of the fitted distribution for border seed numbers 15 and 3000 are depicted in Fig. 3.

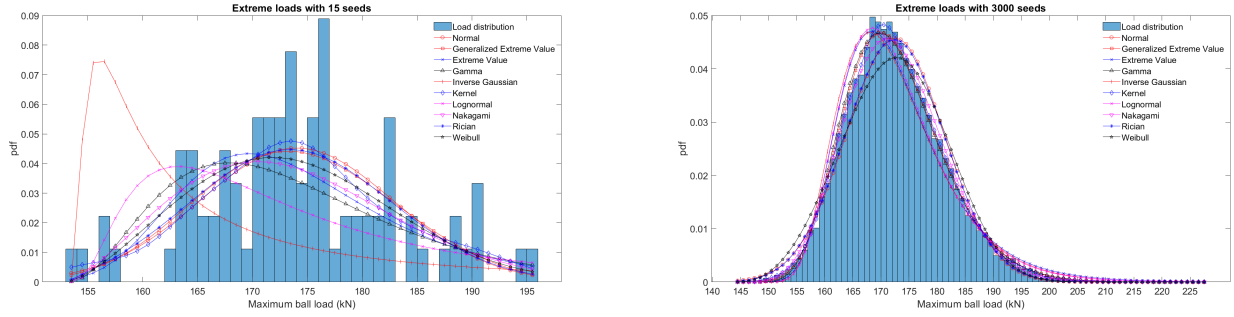

Figure 3. Annual probability density function of different distribution functions in 15 seeds (left) and 3000 seeds (right)

CE indicator results in different seed numbers with nominated probability distribution functions are presented in Table 6

Table 6. Coefficient of efficiencies of the nominated probability distribution functions in different seed numbers

PDF	CE														
	15	30	50	75	100	150	200	300	600	900	1200	1500	1800	2400	3000
Nor	0.464	0.677	0.793	0.753	0.871	0.872	0.944	0.942	0.961	0.961	0.972	0.971	0.977	0.977	0.977
GEV	0.461	0.672	0.858	0.807	0.921	0.914	0.974	0.972	0.982	0.982	0.993	0.994	0.994	0.995	0.996
EV	0.409	0.587	0.855	0.814	0.911	0.906	0.951	0.949	0.953	0.953	0.970	0.975	0.970	0.971	0.976
Gam	0.307	0.517	0.846	0.812	0.912	0.913	0.958	0.963	0.970	0.970	0.985	0.993	0.984	0.988	0.995
IG	-1.218	-0.685	0.614	-0.169	0.802	0.791	0.818	0.805	0.860	0.860	0.911	0.965	0.904	0.932	0.968
Ker	0.510	0.703	0.867	0.836	0.928	0.920	0.977	0.975	0.989	0.989	0.997	0.997	0.997	0.999	0.999
LN	0.023	0.262	0.767	0.691	0.865	0.883	0.899	0.921	0.927	0.927	0.949	0.977	0.946	0.957	0.978
Nak	0.392	0.613	0.852	0.822	0.913	0.909	0.969	0.966	0.978	0.978	0.990	0.990	0.992	0.993	0.994
Ric	0.459	0.667	0.834	0.791	0.888	0.881	0.953	0.948	0.965	0.965	0.977	0.974	0.981	0.980	0.979
Wbl	0.429	0.641	0.846	0.812	0.897	0.883	0.955	0.939	0.955	0.955	0.971	0.957	0.975	0.971	0.964

https://doi.org/10.5194/wes-2024-186
Preprint. Discussion started: 23 January 2025

eawe european academy of wind energy
Open Access WIND ENERGY SCIENCE DISCUSSIONS

The results show that the kernel and generalized extreme value best perform in modeling the extreme load distribution. This dominance started with 150 seeds. The kernel estimator does not have a closed formula, and the generalized extreme value is considered a distribution for modeling the effect of seed number in the distribution of extreme loads. The results also indicate that a low number of seed values cannot accurately represent the true variety of the extreme loads.

230 Changes in the mean of the GEV function due to the seed number are plotted in Fig. 4.

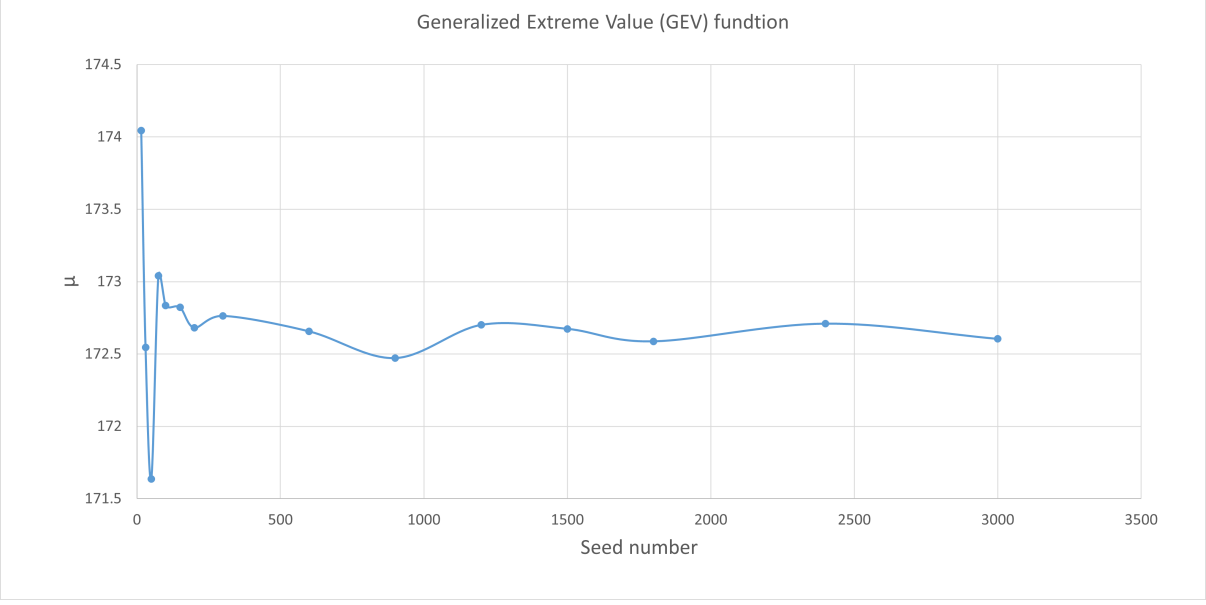

Figure 4. Changes of mean of generalized extreme value distribution due to seed numbers

It is very time-consuming to consider the high number of random seeds in the simulations. In addition, changes in the GEV parameters in 300 seeds and more are less than 3%. The 300 seed number is the value that is considered for the random seed number in the rest of the results.

4.2 Sensitivity analysis

235 The probability of failure (Pf) in the bearing with variation in the ball diameter, pitch circle diameter, conformity, and contact angle is studied. The onshore wind field with a turbulence intensity grade of IA according to IEC 61400 is considered. 10^8 samples were considered in the simulation with the Monte Carlo method, and this process was repeated 20 times. It is observed that raceway conformity has the dominant effect on blade bearing failure in ULS. Consequently, the uncertainty of the raceway conformity with normal distribution with a standard deviation of %0.5 for the uncertainty of dimension, χ_d, is considered.

https://doi.org/10.5194/wes-2024-186
Preprint. Discussion started: 23 January 2025

eawe european academy of wind energy
Open Access WIND ENERGY SCIENCE DISCUSSIONS

4.2.1 Ball diameter

The nominal size of the ball diameter is 75 mm. It is assumed that the ball diameter can change from fine to very coarse machining according to ISO 2768-1 ISO 2768-1 (1989). It leads to a 0.15 to 1.5 mm variation in the ball diameter. The failure probability of the bearing with different ball diameters is shown in Fig. 5a. Increasing the ball diameter increases the reliability of the bearing, which is in good agreement with the results from Wang and Zhang (2022); however, the reliability decreases more sharply in their analysis.

4.2.2 Pitch circle diameter

The nominal size of the pitch circle diameter is 3558 mm. It is assumed that the pitch circle diameter can change from medium (2 mm) to very coarse (8 mm) machining according to ISO 2768-1 (1989). In order to observe the wider range of diameters, diameters of 3540 and 3576 mm were added to the study. The failure probability of the bearing with different pitch circle diameters is shown in Fig. 5b. The results show that the pitch circle diameter does not have a significant effect on the Pf.

4.2.3 Raceway conformity

Raceway conformity is the dimensional relationship between the radius of the raceway and the diameter of the ball. The nominal size of the conformity in the current study is 0.53. According to Daidié et al. (2008), bearing manufacturers recommend a value between 0.510 and 0.543 for this ratio. In this study, the conformity between 0.515 and 0.545 is studied. The failure probability of the bearing with different raceway conformities is shown in Fig. 5c. The results of the Pf show that with an increase in conformity, reliability sharply decreases. Wang and Zhang (2022) reached the same conclusion, but the decrease in reliability was not as sharp as the results presented. Wang et al. (2016) got the same results in the maximum Hertzian contact stress in their research for angular contact ball bearings. In order to understand how much the manufacturing of the ball and raceway can affect the reliability of the bearing, it is assumed that the ball and raceways have a fine degree of manufacturing according to ISO 2768-1 (1989), where in our study the tolerance would be 0.15 mm and the extreme values for conformity would be 0.527 and 0.533. The extreme values for the raceway conformity by this assumption are shown with vertical lines in Fig. 5c.

4.2.4 Contact angle

The nominal size of the initial contact angle is 45 degrees. The contact angle from 25 °to 65 °is studied. The failure probability of the bearing with different contact angles is shown in Fig. 5d. The results show that the probability of failure decreases by increasing the contact angle. Cheng et al. (2020) got the same results in the shear stress in their research for angular contact ball bearings.

https://doi.org/10.5194/wes-2024-186
Preprint. Discussion started: 23 January 2025

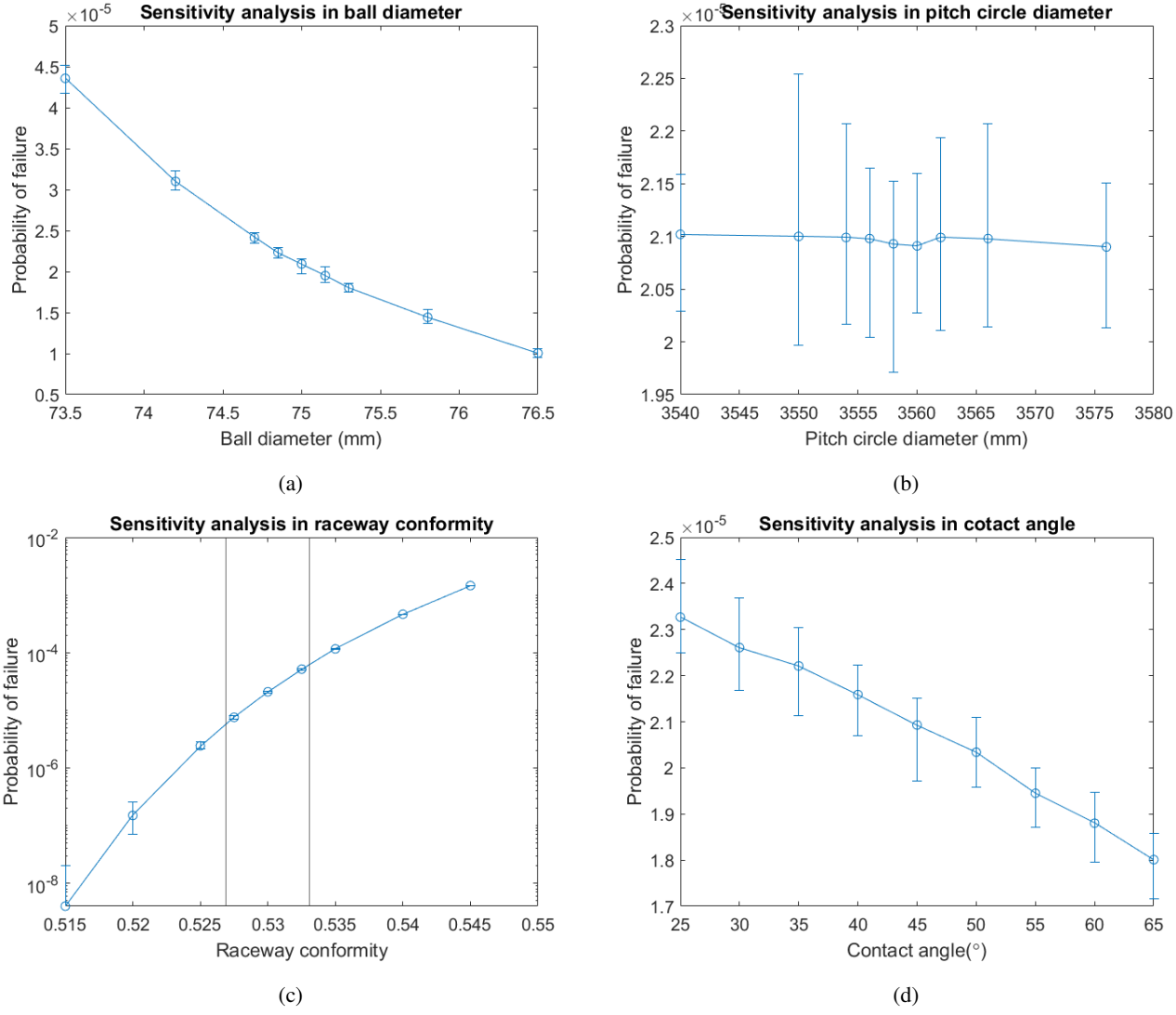

Figure 5. The probability of failure with different (a) ball diameter, (b) pitch circle diameter, (c) raceway conformity, (d) contact angle

4.3 IEC wind conditions

The IEC wind categories I, II, and III in the turbulence intensity of A, B, and C at onshore and offshore conditions are studied. Simulations with different numbers of samples were performed. the result of the Pf in IEC class I is depicted in Fig. 6.

https://doi.org/10.5194/wes-2024-186
Preprint. Discussion started: 23 January 2025

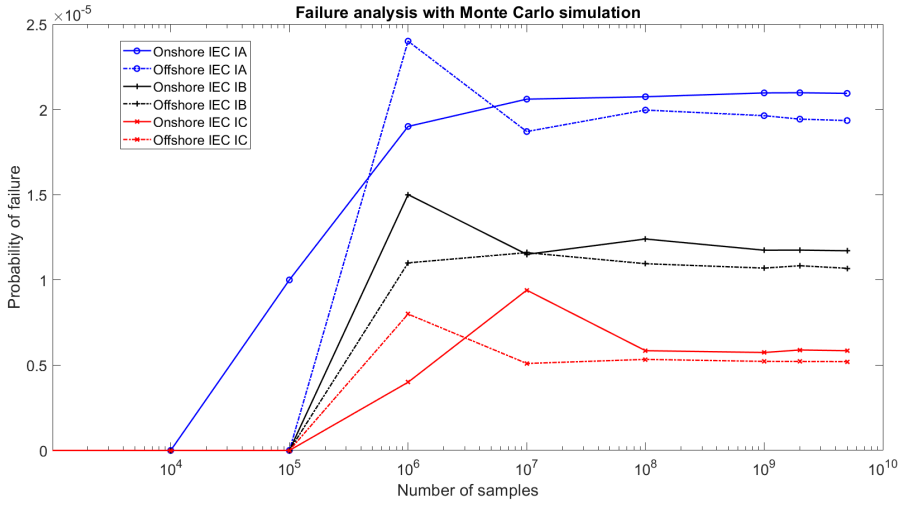

Figure 6. ULS probability of failure of IEC class I wind conditions in different sample numbers in Monte Carlo simulation

As the results show, the Pf converges after 10^7 samples in all wind conditions. To account for a wide range of samples, 10^8 samples were considered in the simulation with the Monte Carlo method, which was repeated 20 times (20 clusters of 10^8 samples). The Pf is the average of 20 clusters. The IEC wind condition probability of failure is illustrated in Fig. 7.

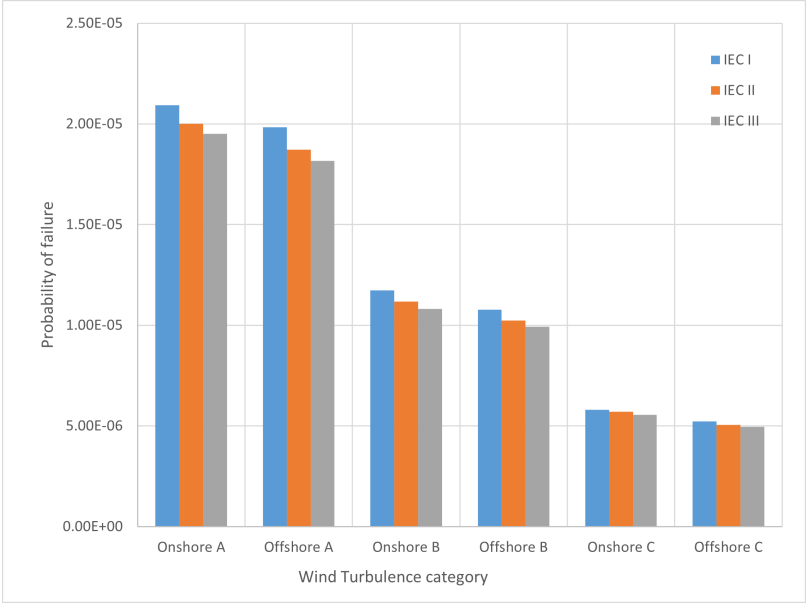

Figure 7. ULS annual probability of failure of IEC wind conditions

https://doi.org/10.5194/wes-2024-186
Preprint. Discussion started: 23 January 2025

eawe european academy of wind energy
Open Access WIND ENERGY SCIENCE DISCUSSIONS

IEC onshore A class IA has a reliability of 0.999979, which is the lowest, and the overall probabilities of failures of IEC wind configurations are in the order of 10^{-5}. By increasing the annual mean wind speed, reliability decreases; however, the turbulence intensity has a more significant effect, and reliability decreases when the turbulence intensity increases. While the Pf mean value varies between 2.09×10^{-5} and 4.95×10^{-6}, the standard deviation of the clusters varies between 5.56×10^{-7} and 1.9×10^{-7}. The variance of the results is too small, and it indicates that the clusters are closer together, suggesting less diversity and more consistency.

IEC 61400-1 (2019) recommends 15 seed numbers in the ultimate analysis. It is shown that 15 seed numbers cannot represent the behavior of the probability distribution of the extreme loads. To investigate further, the load index is introduced. The load index is the ratio of the extreme ball loads in 300 seed numbers to the extreme ball loads in 15 seed numbers. The load index results of IEC wind categories are plotted in Fig. 8. The results show that the extreme load calculation with 15 seeds has an error between 2% and 11%.

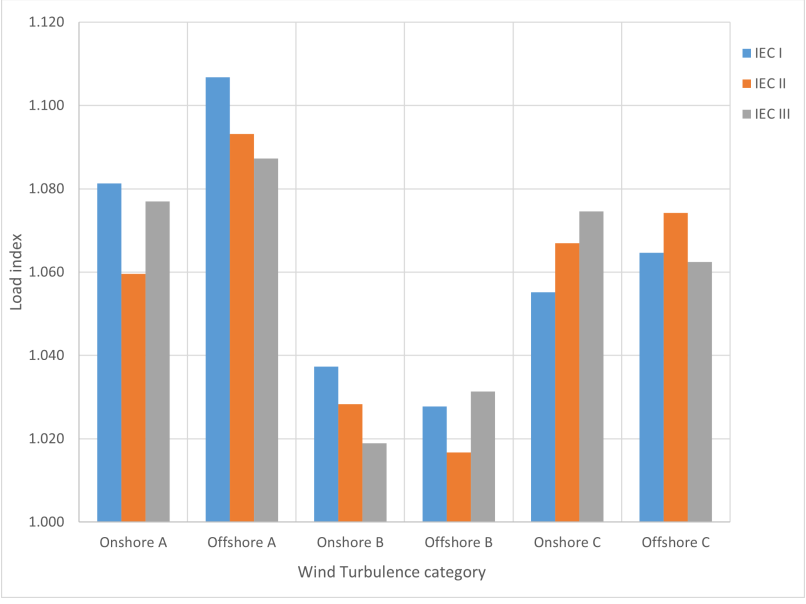

Figure 8. Load index of IEC wind conditions

4.4 Wind sites

The wind sites that were introduced previously were studied. The nominated wind site probability of failures is illustrated in Fig. 9. To compare the results with the IEC wind condition, the maximum of the Pf in the IEC wind condition is added to the figure.

https://doi.org/10.5194/wes-2024-186
Preprint. Discussion started: 23 January 2025

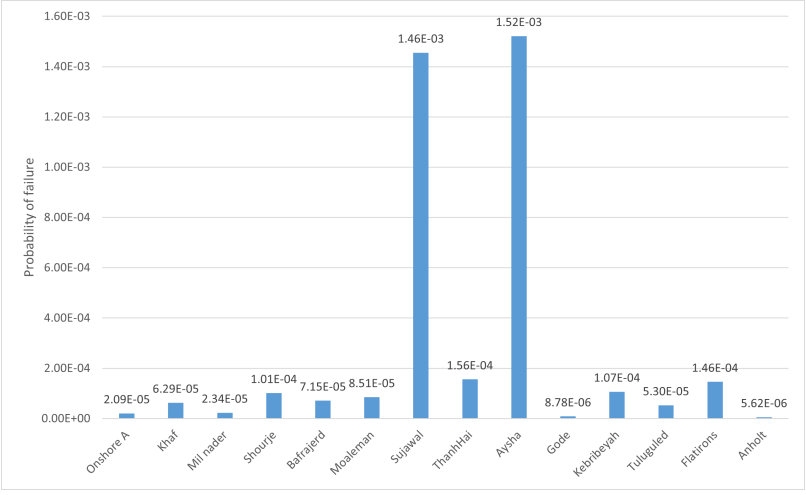

Figure 9. ULS annual probability of failure of nominated wind sites

The results show that most wind sites have a higher probability of failure in ULS in the blade bearing than the IECs. The reliability at the Sujawal and Aysha wind sites is far lower than that of the IEC. The standard deviation of the clusters varies between 4.82×10^{-6} and 2.33×10^{-7}, and the results of the clusters are consistent. These two wind sites have annual wind speeds between 7.5 and 8.5 and are categorized in the IEC II class, while their Pf is higher than the IEC I class wind sites. The load index results of wind sites are plotted in Fig. 10.

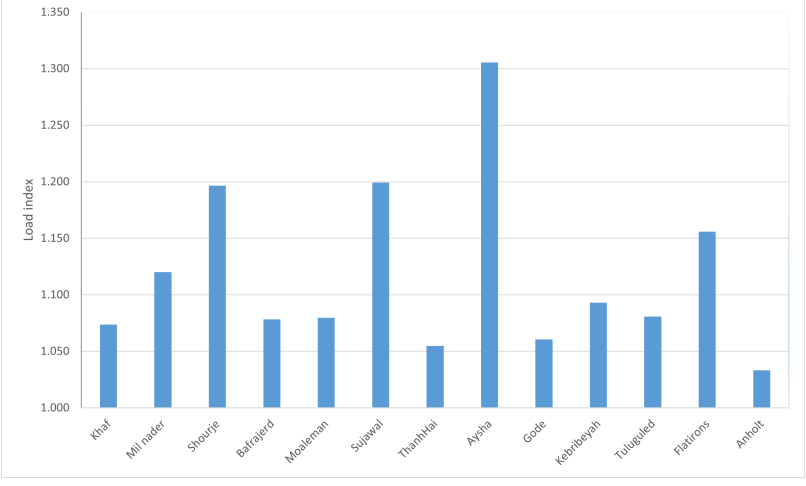

Figure 10. Load index of wind sites

The results show that the extreme load calculation with 15 seeds has an error between 3% and 30%.

https://doi.org/10.5194/wes-2024-186
Preprint. Discussion started: 23 January 2025

eawe european academy of wind energy
Open Access WIND ENERGY SCIENCE DISCUSSIONS

5 Conclusions

The presented work studies the probability of failure in the blade bearing at the ultimate limit state. The static safety factor, which is the ratio between the maximum permissible Hertzian contact stress and the maximum contact stress, is considered for calculating the probability of failure. The NREL 5 MW reference wind turbine is considered with the extreme turbulence wind model in the design load case. The Monte Carlo method was used to calculate the probability of failure.

It is shown that the generalized extreme value is a suitable function to simulate the probability of the extreme ball load distribution. By increasing the number of seeds in simulating the turbulence model, the accuracy of the probability function increased. It is observed that by considering 15 seed numbers, as proposed in the standards and guidelines, the effect of different turbulence conditions cannot be achieved.

The probability of failures of the blade bearing regarding variations of four main dimensions was studied. Ball diameter and raceway conformity in this aspect have the highest contribution to the reliability of the blade bearing, and strictly controlling these parameters can lead to higher reliability in the bearing regarding the ultimate limit state.

The pf results of different IEC wind conditions show that the IEC IA onshore category has the highest probability of failure, and the IEC IIIA offshore category has the lowest. However, the effect of wind class (I, II, III) and onshore and offshore is not considerable in the probability of failure; turbulence intensity (A, B, C) has a significant effect on the reliability. The probability of failure for the selected onshore and offshore wind sites are mostly worse than those of IEC sites, which indicates that IEC designed turbines may result in lower blade bearing reliability and shorter life if are used in those wind sites.

Code and data availability. The code and data used in this study is available upon reasonable request.

Author contributions. AR wrote the original draft. ARN contributed to paper revisions, funding acquisition.

Competing interests. ARN is a member of the editorial board of the Wind Energy Science journal. The authors declare that they have no further conflicts of interest.

Acknowledgements. This research was partially supported by Made4Wind project Under Horizon Europe Research and innovation funding programme under GA No. 101136096.

https://doi.org/10.5194/wes-2024-186
Preprint. Discussion started: 23 January 2025

eawe european academy of wind energy
Open Access WIND ENERGY SCIENCE DISCUSSIONS

References

Alavi, O., Mohammadi, K., and Mostafaeipour, A.: Evaluating the suitability of wind speed probability distribution models: A case of study of east and southeast parts of Iran, Energy Conversion and Management, 119, 101–108, https://doi.org/10.1016/j.enconman.2016.04.039, 2016.

Andreasen, D. K., Rodenas-Soler, C., Oertel, U., Krugel, K., Reinares, I., Mendia, I. S., Nielsen, J. H., Olsen, A., Tinni, A., Vizireanu, D., Cheaytani, J., Kratz, M., and Bousseau, P.: Portability of failure mode detection/prognosis orientations 2.0, Tech. rep., ROMEO, https://www.romeoproject.eu/wp-content/uploads/2022/10/D2_4_Portability_2_3_final.pdf, 2022.

Bain, L. J. and Antle, C. E.: Estimation of Parameters in the Weibull Distribution, Technometrics, 9, 621–627, 1967.

Cheng, H., Zhang, Y., Lu, W., and Yang, Z.: Reliability sensitivity analysis based on stress–strength model of bearing with random parameters, Review of Scientific Instruments, 91, 073 908, https://doi.org/10.1063/1.5143405, 2020.

Daidié, A., Chaib, Z., and Ghosn, A.: 3D Simplified Finite Elements Analysis of Load and Contact Angle in a Slewing Ball Bearing, Journal of Mechanical Design, 130, 082 601, https://doi.org/10.1115/1.2918915, 2008.

Dawson, C., Abrahart, R., and See, L.: HydroTest: a web-based toolbox of evaluation metrics for the standardised assessment of hydrological forecasts, Environmental Modelling & Software, 22, 1034–1052, https://doi.org/10.1016/j.envsoft.2006.06.008, 2007.

Ditlevsen, O. and Madsen, H.: Structural Reliability Methods, Technical University of Denmark, https://books.google.no/books?id=Z1LOPwAACAAJ, 2007.

DNV-ST-0437: Loads and site conditions for wind turbines, 2016.

Germanischer Lloyd: Guideline for the Certification of Wind Turbines, 2010.

GIZ: Vietnam - Wind Measurement Data, https://energydata.info/dataset/vietnam-wind-measurements-giz, [Online; accessed 20-January-2023], 2023.

Graßmann, M., Schleich, F., and Stammler, M.: Validation of a finite-element model of a wind turbine blade bearing, Finite Elements in Analysis and Design, 221, 103 957, https://doi.org/https://doi.org/10.1016/j.finel.2023.103957, 2023.

Harris, T., Rumbarger, J., and C.P., B.: Wind Turbine Design Guideline DG03: Yaw and Pitch Rolling Bearing Life, Tech. rep., NREL/TP-500-42362, National Renewable Energy Lab.(NREL), Golden, CO (United States), https://doi.org/10.2172/969722, 2009.

Harris, T. A. and Kotzalas, M. N.: Rolling bearing analysis-2 volume set, Crc Press, 2006.

IEA: Renewable Energy Market Update Outlook for 2023 and 2024, Tech. rep., International Energy Agency (IEA), https://www.iea.org/reports/renewable-energy-market-update-june-2023, 2023.

IEC 61400-1: Wind energy generation system, part 1: Design requirements, https://webstore.iec.ch/publication/26423, 2019.

ISO 19902: Petroleum and natural gas industries — Fixed steel offshore structures, https://www.iso.org/standard/65688.html, 2020.

ISO 19904-1: Petroleum and natural gas industries — Floating offshore structures, Part 1: Ship-shaped, semi-submersible, spar and shallow-draught cylindrical structures, https://www.iso.org/standard/63801.html, 2019.

ISO 2394: General principles on reliability for structures, https://www.iso.org/standard/58036.html, 2015.

ISO 2768-1: General tolerances- Part 1: Tolerances for linear and angular dimensions without individual tolerance indications, ISO, https://www.iso.org/standard/7748.html, 1989.

ISO 76: Rolling bearings — Static load ratings, https://www.iso.org/standard/38101.html, 2006.

Jager, D. and Andreas, A.: NREL National Wind Technology Center (NWTC): M2 Tower; Boulder, Colorado (Data);, Tech. rep., NREL Report No. DA-5500-56489, https://doi.org/10.5439/1052222, 1996.

https://doi.org/10.5194/wes-2024-186
Preprint. Discussion started: 23 January 2025

Jonkman, B.: TurbSim User's Guide: Version 1.50, Tech. rep., NREL/TP-500-46198, National Renewable Energy Lab.(NREL), Golden, CO (United States), https://doi.org/10.2172/965520, 2009.

Jonkman, J., Butterfield, S., Musial, W., and Scott, G.: Definition of a 5-MW reference wind turbine for offshore system development, Tech. rep., National Renewable Energy Lab.(NREL), Golden, CO (United States), https://doi.org/10.2172/947422, 2009.

Keller, J. and Guo, Y.: Rating of a Pitch Bearing for a 1.5-MW Wind Turbine, Tech. rep., NREL/TP-5000-82462, National Renewable Energy Lab.(NREL), Golden, CO (United States), https://doi.org/10.2172/1902646, 2022.

Leupold, S., Schelenz, R., and Jacobs, G.: Method to determine the local load cycles of a blade bearing using flexible multi-body simulation, Forsch. Ingenieurwes, 85, 211–218, https://doi.org/https://doi.org/10.1007/s10010-021-00457-y, 2021.

Lewis, S., Gaillard, L., Seiler, R., Parzianello, G., and LeLetty, R.: Recent Steps Towards a Common Understanding of Ball Bearing Load Capacity, in: ESA Special Publication, edited by Ouwehand, L., vol. 737 of *ESA Special Publication*, p. 35, 2015.

Melchers, R. E. and Beck, A. T.: Structural reliability analysis and prediction, John wiley & sons, 2018.

Menck, O., Stammler, M., and Schleich, F.: Fatigue lifetime calculation of wind turbine blade bearings considering blade-dependent load distribution, Wind Energy Science, 5, 1743–1754, https://doi.org/10.5194/wes-5-1743-2020, 2020.

Nejad, A. R.: Modelling and analysis of drivetrains in offshore wind turbines, Offshore wind energy technology, 37, 2018.

Rezaei, A. and Nejad, A. R.: Effect of wind speed distribution and site assessment on pitch bearing loads and life, Journal of Physics: Conference Series, 2507, 012 021, https://doi.org/10.1088/1742-6596/2507/1/012021, 2023.

Rezaei, A., Guo, Y., Keller, J., and Nejad, A. R.: Effects of wind field characteristics on pitch bearing reliability: a case study of 5 MW reference wind turbine at onshore and offshore sites, Forschung im Ingenieurwesen, 87, 321–338, 2023.

Rezaei, A., Schleich, F., Menck, O., Grassmann, M., Bartschat, A., and Nejad, A. R.: Comparative analysis of rolling contact fatigue life in a wind turbine pitch bearing with different modeling approaches, in: Journal of Physics: Conference Series, vol. 2767, p. 052036, IOP Publishing, 2024.

SATBA, R.: http://www.satba.gov.ir/en/, [Online; accessed 24-May-2022], 2022.

Shi, H., Z. Dong, N. X., and Huang, Q.: Wind Speed Distributions Used in Wind Energy Assessment: A Review, Frontiers in Energy Research, 9, 769 920, 2021.

Shimizu, S., Tosha, K., and Tsuchiya, K.: New data analysis of probabilistic stress-life (P–S–N) curve and its application for structural materials, International Journal of Fatigue, 32, 565–575, https://doi.org/10.1016/j.ijfatigue.2009.07.017, 2010.

Stammler, M., Menck, O., Guo, Y., and Keller, J.: Wind Turbine Design Guideline DG03: Yaw and Pitch Bearings, Tech. rep., NREL/TP-5000-89161, National Renewable Energy Lab.(NREL), Golden, CO (United States), https://doi.org/https://doi.org/10.2172/2406870, 2024.

Stehly, T., Duffy, P., and Hernando, D. M.: 2022 Cost of Wind Energy Review, Tech. rep., NREL/PR-5000-88335, National Renewable Energy Lab.(NREL), Golden, CO (United States), https://doi.org/10.2172/969722, 2023.

Wang, X. and Zhang, T.: Plastic deformation-based rolling bearing reliability and sensitivity analysis under incomplete probability information, Advances in Mechanical Engineering, 14, 16878132221142 968, https://doi.org/10.1177/16878132221142968, 2022.

Wang, X., Wang, B., Chang, M., and Li, L.: Reliability and sensitivity analysis for bearings considering the correlation of multiple failure modes by mixed Copula function, Proceedings of the Institution of Mechanical Engineers, Part O: Journal of Risk and Reliability, 234, 15–26, https://doi.org/10.1177/1748006X19876137, 2020.

Wang, Y., Wang, W., and Zhao, Z.: Effect of race conformities in angular contact ball bearing, Tribology International, 104, 109–120, https://doi.org/10.1016/j.triboint.2016.08.034, 2016.

https://doi.org/10.5194/wes-2024-186
Preprint. Discussion started: 23 January 2025

World Bank Group: Ethiopia - Wind Measurement Data, https://energydata.info/dataset/ethiopia-wind-measurement-data, [Online; accessed 20-January-2023], 2023a.

World Bank Group: Pakistan - Wind Measurement Data, https://energydata.info/dataset/pakistan-wind-measurement-data, [Online; accessed 20-January-2023], 2023b.

Yu, J., Fu, Y., Yu, Y., Wu, S., Wu, Y., You, M., Guo, S., and Li, M.: Assessment of Offshore Wind Characteristics and Wind Energy Potential in Bohai Bay, China, Energies, 12, https://doi.org/10.3390/en12152879, 2019.

Ørsted: Green solutions: Offshore wind data, https://orsted.com/en/our-business/offshore-wind/wind-data, [Online; accessed 4-June-2022], 2022.